Compactness of Neutron Stars

Wei-Chia Chen and J. Piekarewicz

On the compactness of neutron stars

Wei-Chia Chen[1, *] and J. Piekarewicz[1, †]

[1]*Department of Physics, Florida State University, Tallahassee, FL 32306*
(Dated: September 24, 2015)

Recent progress in the determination of both masses and radii of neutron stars are starting to place stringent constraints on the dense matter equation of state. In particular, new theoretical developments together with improved statistical tools seem to favor stellar radii that are significantly smaller than those predicted by models using purely nucleonic equations of state. Given that the underlying equation of state must also account for the observation of $2M_\odot$ neutron stars, theoretical approaches to the study of the dense matter equation of state are facing serious challenges. In response to this challenge, we compute the underlying equation of state associated with an assumed mass-radius template similar to the "common radius" assumption used in recent studies. Once such a mass-radius template is adopted, the equation of state follows directly from the implementation of Lindblom's algorithm; assumptions on the nature or composition of the dense stellar core are not required. By analyzing mass-radius profiles with a maximum mass consistent with observation and common radii in the 8 to 11 km range, a lower limit on the stellar radius of a $1.4M_\odot$ neutron star of $R_{\rm NS} \gtrsim 10.7$ km is required to prevent the equation of state from violating causality.

How does subatomic matter organize itself and what phenomena emerge is one of the overarching questions guiding the field of nuclear physics [1]. In the case of atomic nuclei, the quest to answer this question requires understanding the nature of the nuclear force and the limits of nuclear existence. In the case of extended nucleonic matter, this involves elucidating the nature of neutron stars and dense nuclear matter. In this letter we focus on the latter.

Owing to the long-range nature of the Coulomb force, extended nucleonic matter must be electrically neutral. As a result, dense nuclear matter must be by necessity neutron-rich. This is because the electronic contribution to the energy increases rapidly with density, so electron capture becomes energetically advantageous. Given that such extreme conditions of density and isospin asymmetry can not be realized in terrestrial experiments, neutron stars have become unique laboratories for the exploration of dense matter. This situation has created a strong synergy between nuclear physics and astrophysics, that has been cemented even further through an intimate interplay between theory, experiment, and observation [2]. Indeed, powerful telescopes operating at a variety of wavelengths drive new theoretical and experimental efforts which in turn suggest new observations.

A recent example of such a unique synergy is how accurate measurements of massive neutron stars [3, 4] have informed nuclear models that fall under the general rubric of density functional theory. Density functional theory (DFT) offers a comprehensive—and likely unique—framework to describe strongly interacting nuclear many-body systems ranging from finite nuclei to neutron stars. Rooted on the seminal work by Kohn and collaborators [5], DFT shifts the focus from the complicated many-body wave function to the much simpler one-body density. The implementation of DFT to nuclear physics requires that the parameters of the model—which encode some of the complicated many-body dynamics—be determined by fitting directly to experimental data. In this regard, the accurate measurement of neutron star masses has been vital to the accurate calibration of some modern energy density functionals [6–8].

Whereas the determination of neutron star masses is accurate and beyond question, attempts to reliably extract stellar radii [9–11] have been hindered by large systematic uncertainties that resulted in an enormous disparity in stellar radii—ranging from as low as 8 km [9] all the way to 14 km [11]. It appears, however, that since those first analyzes were performed, the situation has significantly improved in the last few years through a better understanding of systematic uncertainties, important theoretical developments, and the implementation of robust statistical methods [12–16]. Although a consensus has yet to be reached, these recent studies seem to favor stellar radii in the 9–11 km range. Particularly intriguing among these are the results by Guillot and collaborators that suggest a "common radius" of $R_{\rm NS} = 9.1^{+1.3}_{-1.5}$ km for all five quiescent low mass x-ray binaries used in their analysis [12]; this common-radius value has been slightly revised to $R_{\rm NS} = (9.4 \pm 1.2)$ km [15]. What makes this result especially provocative is that satisfying the small radius and large mass constraints simultaneously is enormously challenging. Indeed, to our knowledge no optimized energy density functional can simultaneously reproduce both of these constraints. And from the very large number of models available in the literature [17], we are aware of only a few that account for both [18–20]. From these, the model due to Wiringa, Fiks, and Fabrocini [18] relies on a microscopic approach based on the Argonne v_{14} (AV14) nucleon-nucleon potential sup-

plemented with the Urbana VII (UVII) three-nucleon potential. This model predicts a maximum stellar mass of $2.13\,M_\odot$ and a "common radius" of $R_{\rm NS} \simeq 10.4\,{\rm km}$. The other theoretical approach due to Hebeler and collaborators [19, 20] is also microscopic in nature, but instead uses nuclear interactions derived from chiral effective field theory. In particular, their softest equation of state is consistent with the $\sim 2M_\odot$ limit and predicts a radius as low as $R_{1.4} = 9.7\,{\rm km}$ for a $1.4M_\odot$ neutron star [20].

In this letter we aim to elucidate the nature of neutron star matter by relying on a powerful result first proven by Lindblom more than two decades ago [21]. It is a well known fact that all stellar profiles may be determined from the Tolman-Oppenheimer-Volkoff (TOV) equations once an equation of state $P = P(\mathcal{E})$ relating the pressure P to the energy density $\mathcal{E}$ is supplied. That is, given an equation of state (EOS), the TOV equations

$$\frac{dP(r)}{dr} = -\frac{G}{c^2} \frac{\left(\mathcal{E}(r) + P(r)\right)\left(M(r) + \frac{4\pi r^3 P(r)}{c^2}\right)}{r^2\left(1 - \frac{2GM(r)}{c^2 r}\right)}, \quad (1a)$$

$$\frac{dM(r)}{dr} = \frac{4\pi r^2 \mathcal{E}(r)}{c^2}, \quad (1b)$$

can be solved once a value for the central pressure $P(0) = P_c$ and enclosed mass $M(0) = 0$ are specified at the origin. In particular, the stellar radius R is determined from the condition $P(R) = 0$ and the corresponding stellar mass as $M = M(R)$. In this manner, the EOS generates the mass-radius (MR) relationship for neutron stars. What Lindblom was able to prove and implement is that the inverse also holds true: knowledge of the MR relation *uniquely* determines the neutron star matter equation of state [21].

In the spirit of Lindblom's approach, we now proceed to outline the methodology required to obtain the unique equation of state associated with an assumed MR template that closely resembles the "common-radius" hypothesis adopted in Ref. [12]. This choice of template is the only model assumption made in this work; no additional assumptions on the nature or composition of dense matter are required. For alternative attempts at obtaining generic model-independent constraints see Ref. [22] and references contained therein.

The particular MR template adopted in this work follows from our latest optimization: a relativistic energy density functional labeled "FSUGarnet" [8]. Such a template, among many others depicted in Fig.1, is displayed with the purple solid line containing a few additional circles. FSUGarnet was optimized with inputs from the ground-state properties of finite nuclei, their monopole response, and a maximum neutron star mass consistent with observation. Yet, even after such an optimization, extrapolations to the high-density domain remain highly uncertain. However, it is worth underscoring that relativistic density functionals provide a Lorentz covariant—

and hence causal—framework that becomes critical as one extrapolates to the high densities encountered in the stellar interior. Of particular relevance to this work are predictions for the maximum neutron star mass and radius of a $1.4M_\odot$ neutron star; FSUGarnet predicts: $M_{\rm max} = (2.07 \pm 0.02)\,M_\odot$ and $R_{1.4} = (13.0 \pm 0.1)\,{\rm km}$. Although such a stellar radius appears to significantly exceed some of the preferred limits, the predicted EOS is relatively soft in the immediate vicinity of nuclear matter saturation density. This is relevant as the pressure in the neighborhood of twice nuclear matter saturation density sets the overall scale for stellar radii [17].
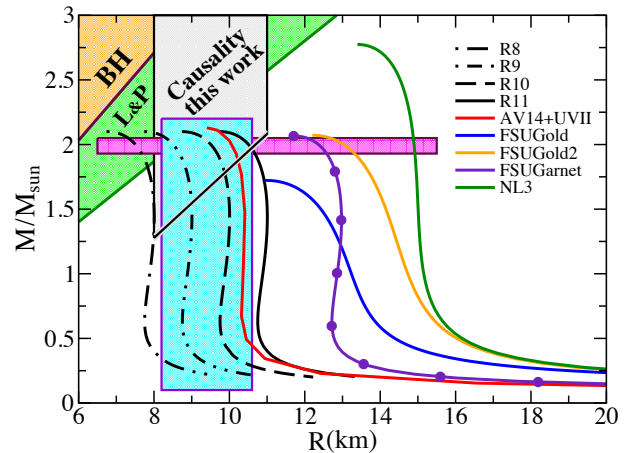

FIG. 1: (Color online) Mass-Radius profiles as predicted by the microscopic model of Ref. [18] and by the four relativistic density functionals considered in the text. As a check, the circles on top of the FSUGarnet profile were obtained using an EOS extracted from Lindblom's algorithm. Also shown are the four profiles R8–R11 generated from the FSUGarnet template and having radii of 8–11 km, respectively. The horizontal band shows the observational constraints from the mass measurements reported in Refs. [3, 4], whereas the vertical band displays the constraint on stellar radii published in [15]. Also shown are regions excluded on purely theoretical grounds: BH is the black hole limit, L&P is the causality constraint obtained in Ref. [17], and the grey region defines the causality constraint obtained in this work.

Having defined the underlying template, additional MR curves may be easily generated by simply shifting the full FSUGarnet profile to the desired radius. Indeed, the curves labeled R8–R11 in Fig. 1 were generated in precisely this manner and are characterized by stellar radii of 8–11 km (rather than 13 km) for a $1.4M_\odot$ neutron star. In the case of these four curves, the underlying EOS is unknown. Besides the FSUGarnet template, MR predictions generated with other relativistic density functionals are also included for comparison. These range from NL3 [23, 24] and FSUGold [25] that were optimized without incorporating neutron star information, to the more recent FSUGold2 parametrization that includes the $2M_\odot$ constraint in the calibration [7]. Note that all these functionals provide accurate descriptions of a variety of

ground-state properties of finite nuclei. Finally, displayed with the red line is the MR relation predicted by the microscopic formalism of Wiringa, Fiks, and Fabrocini [18]. With the exception of FSUGold, all MR relations are consistent with the $2M_\odot$ limit depicted in the figure with the narrow magenta band. However, none of the relativistic density functionals satisfy the common-radius constraint of Ref. [15] depicted in Fig. 1 by the vertical (cyan) band.

Our next step is to use Lindblom's approach to obtain the EOS corresponding to the R8–R11 profiles displayed in Fig. 1. Briefly, the "inversion" procedure is implemented as follows. First, one assumes complete knowledge of the EOS up to a pressure P_i and energy density $\mathcal{E}_i$ capable of supporting neutron stars up to a mass of about $0.4\,M_\odot$. Specifically, using such an EOS and a central pressure of $P_c = P_i$ one generates, through the TOV equations, a neutron star of mass $M_i \approx 0.4\,M_\odot$ and radius R_i. Second, one steps along the mass-radius trajectory by selecting a neutron star of mass $M_{i+1} > M_i$ and radius R_{i+1} whose central pressure P_c and energy density $\mathcal{E}_c$ are to be determined. To compute P_c and $\mathcal{E}_c$, the TOV equations are integrated inwards from the surface to the core, with boundary conditions given by $P(R_{i+1}) = 0$ and $M(R_{i+1}) = M_{i+1}$. Hydrostatic equilibrium guarantees that as one moves towards the interior of the star, the pressure will continue to increase until the maximum known pressure P_i will be reached at a certain radius r_i located near the center of the star. Given that r_i is close to the origin, one may use suitable series expansions to determine the central pressure P_c and energy density $\mathcal{E}_c$ in terms of known quantities, i.e., mass, pressure, and energy density, at the small radius r_i [21]. In this manner, after one iteration the EOS is extended from $(P_i, \mathcal{E}_i)$ to $(P_{i+1}, \mathcal{E}_{i+1}) \equiv (P_c, \mathcal{E}_c)$. In the next iteration, one proceeds in exactly the same fashion, namely, one moves another step along the mass-radius trajectory and repeats the algorithm with the newly augmented equation of state. After the whole mass-radius trajectory is sampled, the entire high-density component of the equation of state is mapped out. Testing the reliability and accuracy of Lindblom's inversion algorithm is fortunately very simple. To start, one uses a known EOS—such as the one predicted by FSUGarnet—to compute its associated MR relation. Then, one applies Lindblom's algorithm to extract the "new" EOS directly from the MR profile. Finally, one verifies that both the new EOS and the resulting MR profile are consistent with the originals. The result of such a test is illustrated in Fig.1 for the case of FSUGarnet; the circles represent the results obtained with an EOS extracted from Lindblom's algorithm.

Having verified the accuracy of Lindblom's algorithm, we can now obtain the equations of state that generate the R8–R11 MR profiles assumed in Fig. 1. To do so, the low-density component of each of the equations of state needed to initialize Lindblom's algorithm must be adjusted to match smoothly to the assumed MR profile
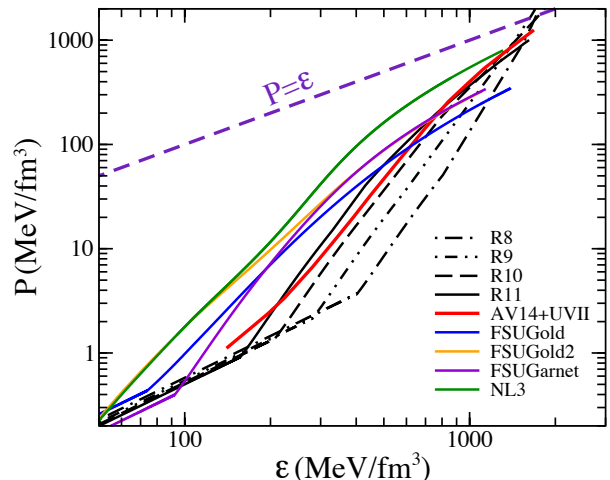

FIG. 2: (Color online) Equations of state associated to the mass-radius profiles displayed in Fig. 1. In the case of the R8–R11 profiles, the equations of state were obtained from Lindblom's algorithm [21]. Also shown is the $P = \mathcal{E}$ line which demarcates the boundary beyond which an equation of state becomes ultrabaric. Equations of state that cross the line become superluminal at considerably lower energy densities.

up to $M \lesssim 0.4\,M_\odot$. Note that at low densities neutron star matter consists of a Coulomb crystal of neutron-rich nuclei (outer crust) followed by the putative "nuclear pasta" (inner crust). In constructing the EOS at low densities, we have relied on the BPS parametrization for all models—including R8–R11. Thus, at very low densities the EOS is the same for all profiles and consistent with known physics. For the nuclear pasta EOS, which remains an open question, we resort to a polytropic treatment of the EOS in that region. The polytropic EOS is then smoothly connected to the high-density EOS generated by Lindblom's algorithm. As in the case of FSUGarnet, such a procedure was validated by ensuring that the extracted EOS reproduces the assumed MR curve. This lends credence to our implementation of the algorithm given that the mapping between the MR profile and the underlying EOS is unique.

The resultant equations of state, along with those predicted by the non-relativistic and relativistic models, are displayed in Fig. 2. Note that among the relativistic density functionals, FSUGarnet displays the softest EOS at low energy densities ($\mathcal{E} \lesssim 200\,\text{MeV/fm}^3$). For reference, FSUGarnet predicts a pressure for pure neutron matter at saturation density of $P_\text{PNM} = (2.60 \pm 0.08)\,\text{MeV/fm}^3$. Given that the pressure in the vicinity of twice nuclear matter saturation density sets the overall scale for stellar radii [17], FSUGarnet generates the mass-radius profile with the smallest radii; in contrast, NL3 with the stiffest EOS generates the largest stellar radii. However, since the maximum neutron star mass is sensitive to the EOS at higher densities, FSUGold (with $M_\text{max} = 1.72\,M_\odot$) becomes the softest beyond $\mathcal{E} \approx 200\,\text{MeV/fm}^3$.

Also displayed in Fig. 2 is the $P = \mathcal{E}$ line which marks the boundary beyond which an equation of state becomes *ultrabaric* [26, 27]. Being rooted on a Lorentz covariant framework, the predictions from all relativistic density functionals lie safely below the ultrabaric line. However, this is not the case for the R8–R11 profiles. Could this be an indication that such profiles violate *causality*? That is, could the speed of sound exceed the speed of light in the high-density cores of these extremely compact stars? To test if a given EOS respects causality, we compute the speed of sound in the medium $c_s^2/c^2 = dP/d\mathcal{E}$ and determine whether a point exists at which the EOS becomes superluminal. Such a point $(P_c, \mathcal{E}_c)$ determines the central pressure and energy density of the heaviest neutron star that can be supported by the given EOS; beyond such a mass, the EOS required to support the star becomes acausal.
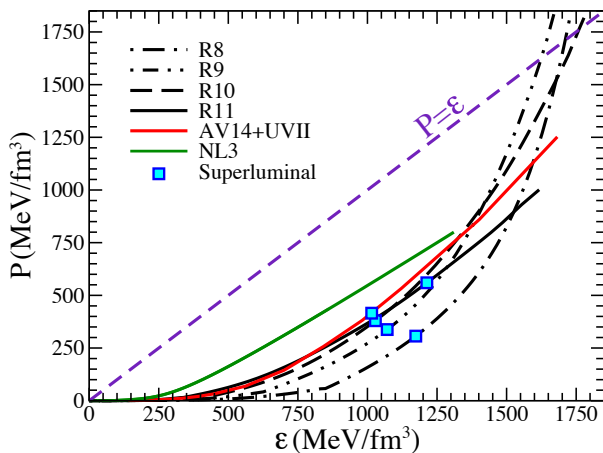

FIG. 3: (Color online) As in Fig. 2, but now on a reduced linear scale, we display some of the equations of state considered in this work; for simplicity, only NL3 is included as a representative member of the relativistic density functionals. With the exception of NL3, which is causal at all densities, all other equations of state become superluminal at the pressure and energy density indicated by the blue squares. In turn, these values determine the central pressure and energy density of the heaviest star that may be supported by a causal EOS.

For clarity, we display in Fig. 3 the various equations of state on a reduced linear scale; only NL3 is included as a representative member of the relativistic density functionals. The figure clearly indicates that with the exception of NL3, all five equations of state become superluminal much before they cross into the ultrabaric region. The pressure and energy density at which the EOS becomes superluminal are depicted by the blue squares. In turn, these values determine the central pressure and energy density of the most massive neutron star that may be supported by a causal EOS; beyond this value the mass-radius relation becomes unphysical. We found that the value of this critical mass $M_{\rm crit}$ decreases rapidly as the common radius decreases. Specifically, although in

the case of the R11 template we find $M_{\rm crit} = 2.06\,M_\odot$, and thus consistent with the present $2M_\odot$ limit [3, 4], we obtain $M_{\rm crit}/M_\odot = 1.83, 1.57, 1.26$, for R10, R9, and R8, respectively. Note that the microscopic model of Wiringa, Fiks, and Fabrocini violates causality beyond $M_{\rm crit} \approx 1.96\,M_\odot$ [18]. These values of $M_{\rm crit}$ define the lower boundary of the grey region labeled as "Causality this work" in Fig. 1. We thus conclude, *within the scope of the adopted MR template*, that in order to satisfy the current $2M_\odot$ limit, the stellar radius of a $1.4M_\odot$ neutron star must exceed 10.7 km. This represents the main finding of our work.

To place our newly developed constraint on the proper context, we display in Fig. 1 two other commonly used limits. The weakest of the two (labeled "BH") represents the black hole limit that precludes a neutron star of mass M from having a radius R equal to its Schwarzschild radius. This constraint has no impact on the mass-radius profiles considered in this work. A more stringent constraint (labeled "L&P") follows from an analysis by Lattimer and Prakash [17, 28] that uses a realistic EOS up to a certain value of the energy density that is then matched to a causally limited EOS. By doing so, they obtain a limit on the stellar compactness that may be written as $R \gtrsim 2.83\,GM/c^2$. Although stronger than the BH constraint, this causality limit does not affect the recent analysis by Guillot and Rutledge [15]. Indeed, the L&P limit for a 9 km neutron star is $2.16\,M_\odot$. On the other hand, our analysis provides an even more stringent constraint of $1.57\,M_\odot$, and pushes the minimum radius to 10.7 km—barely consistent with the upper limit quoted in Ref. [15], but fitting comfortably within the $10.8^{+0.5}_{-0.4}$ km range given in the very recent work by Özel *et al.* [16].

Given that the MR profile is the central assumption made in this work, it is pertinent to ask how sensitive are our conclusions to the underlying shape. As shown in Fig. 4, a constant-radius profile is characterized by a large (indeed infinite) derivative in the mass region of about $0.6 \lesssim M/M_\odot \lesssim 1.6$. If this shape is changed by keeping the slope large but now negative (i.e., an increase in mass is accompanied by a reduction in the radius) then the compactness will increase and the underlying EOS will become superluminal even earlier. However, if instead the slope becomes positive (i.e., an increase in mass is followed by an increase in radius) then it becomes harder to assess whether such an MR profile will generate an acausal EOS; such a shape is displayed by the green solid line in Fig. 4. Still, our results suggest that if variations to the standard template are not overly dramatic, our main conclusions remain valid. Indeed, the minimum stellar radius got shifted by only 0.1 km; from 10.7 to 10.6 km.

In summary, motivated by the latest progress in measuring neutron star radii, which combined with measurements of massive neutron stars provide critical insights into the dense matter equation of state, we have exam-
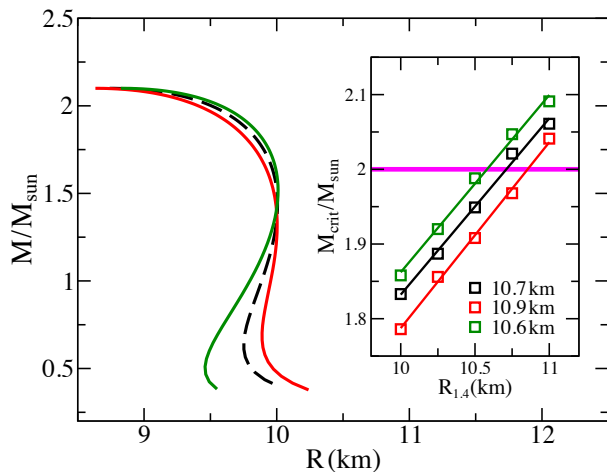
FIG. 4: (Color online) Sensitivity to small variations to the standard MR template. Here the R10 template (dashed line) is modified to produce two additional MR profiles, both with a radius of 10 km for a $1.4 M_\odot$ neutron star. The right portion of the plot displays the critical mass beyond which the underlying EOS becomes superluminal. Finally, the labels indicate the minimum radius required to support a $2 M_\odot$ neutron star with a causal EOS of the given shape.

ined whether neutron stars may be as compact as recently suggested. To do so, we relied on a powerful algorithm developed by Lindblom to obtain the equation of state from knowledge of the mass-radius relationship. That is, given a MR profile, the underlying EOS may be obtained without any assumption on the nature or composition of the dense stellar core. Thus, all model dependence lies in the assumed MR profile, which in the present study was chosen to have a nearly constant radius shape. Using such a template, MR profiles were constructed with a maximum mass of $2.1\,M_\odot$ and with common radii spanning the 8 to 11 km interval. Using Lindblom's algorithm, the equation of state associated with each of these MR profiles was obtained. Further, by imposing causality, namely, by enforcing that the speed of sound be less than the speed of light, we obtained a stringent constraint on the maximum compactness of neutron stars. Indeed, by demanding that a *causal* EOS be able to support a $2 M_\odot$ neutron star, we obtained—*within the scope of the adopted template*—a lower limit on the stellar radius of a $1.4 M_\odot$ neutron star of $R_{\rm NS}^{\rm min} = 10.7$ km. Note that our result imposes a *lower* limit on stellar radii. In contrast, recent observational studies are placing *upper* limits on neutron star radii. We would like to stress that although the EOS of pure neutron matter has been well constrained by theoretical approaches that exploit its close resemblance to a unitary Fermi gas, in this low-density region neutron star matter differs significantly from pure neutron matter because of clustering. Nevertheless, in the future we plan to use existing theoretical and experimental constraints to guide the construction

of the low-mass part of the MR profile and to further explore the sensitivity of our results to the assumed MR profile. We trust that such a theoretical-observational synergy will continue to prove beneficial in the coming years in order to determine the dense matter equation of state.

---

* Electronic address: wc09c@my.fsu.edu
† Electronic address: jpiekarewicz@fsu.edu
[1] *Nuclear Physics: Exploring the Heart of Matter* (The National Academies Press, Washington, 2012).
[2] C. J. Horowitz, E. F. Brown, Y. Kim, W. G. Lynch, R. Michaels, et al., J. Phys. G **41**, 093001 (2014).
[3] P. Demorest, T. Pennucci, S. Ransom, M. Roberts, and J. Hessels, Nature **467**, 1081 (2010).
[4] J. Antoniadis, P. C. Freire, N. Wex, T. M. Tauris, R. S. Lynch, et al., Science **340**, 6131 (2013).
[5] W. Kohn, Rev. Mod. Phys. **71**, 1253 (1999).
[6] J. Erler, C. J. Horowitz, W. Nazarewicz, M. Rafalski, and P.-G. Reinhard, Phys. Rev. C **87**, 044320 (2013).
[7] W.-C. Chen and J. Piekarewicz, Phys. Rev. C **90**, 044305 (2014).
[8] W.-C. Chen and J. Piekarewicz, Phys. Lett. B **748**, 284 (2015).
[9] F. Ozel, G. Baym, and T. Guver, Phys. Rev. D **82**, 101301 (2010).
[10] A. W. Steiner, J. M. Lattimer, and E. F. Brown, Astrophys. J. **722**, 33 (2010).
[11] V. Suleimanov, J. Poutanen, M. Revnivtsev, and K. Werner, Astrophys. J. **742**, 122 (2011).
[12] S. Guillot, M. Servillat, N. A. Webb, and R. E. Rutledge, Astrophys. J. **772**, 7 (2013).
[13] J. M. Lattimer and A. W. Steiner, Astrophys. J. **784**, 123 (2014).
[14] C. O. Heinke, H. N. Cohn, P. M. Lugger, N. A. Webb, W. Ho, et al., Mon. Not. Roy. Astron. Soc. **444**, 443 (2014).
[15] S. Guillot and R. E. Rutledge, Astrophys. J. **796**, L3 (2014).
[16] F. Ozel, D. Psaltis, T. Guver, G. Baym, C. Heinke, et al., arXiv:1505.05155 (2015).
[17] J. M. Lattimer and M. Prakash, Phys. Rept. **442**, 109 (2007).
[18] R. B. Wiringa, V. Fiks, and A. Fabrocini, Phys. Rev. C **38**, 1010 (1988).
[19] K. Hebeler, J. Lattimer, C. Pethick, and A. Schwenk, Phys. Rev. Lett. **105**, 161102 (2010).
[20] K. Hebeler, J. Lattimer, C. Pethick, and A. Schwenk, Astrophys. J. **773**, 11 (2013).
[21] L. Lindblom, Astrophys. J. **398**, 569 (1992).
[22] M. G. Alford, G. Burgio, S. Han, G. Taranto, and D. Zappala, arXiv:1501.07902 (2015).
[23] G. A. Lalazissis, J. Konig, and P. Ring, Phys. Rev. C **55**, 540 (1997).
[24] G. A. Lalazissis, S. Raman, and P. Ring, At. Data Nucl.

Data Tables **71**, 1 (1999).

[25] B. G. Todd-Rutel and J. Piekarewicz, Phys. Rev. Lett. **95**, 122501 (2005).

[26] N. K. Glendenning, *Compact Stars* (Springer-Verlag New York, 2000).

[27] P. Haensel, A. Potekhin, and D. Yakovlev, *Neutron Stars 1: Equation of State and Structure*, Astrophysics and Space Science Library (Springer New York, 2007).

[28] J. M. Lattimer, Annu. Rev. Nucl. Part. Sci. **62**, 485 (2012).